THE JOURNAL OF PHYSICAL CHEMISTRY B
A JOURNAL OF THE AMERICAN CHEMICAL SOCIETY

pubs.acs.org/JPCB

Article

The Curious Case of Aqueous Warfarin: Structural Isomers or Distinct Excited States?

Sushil S. Sakpal,[#] Deborin Ghosh,[#] Meghna A. Manae, Anirban Hazra,* and Sayan Bagchi*

Cite This: *J. Phys. Chem. B* 2021, 125, 2871−2878

Read Online

ACCESS | Metrics & More | Article Recommendations | Supporting Information

ABSTRACT: Warfarin is a potent anti-coagulant drug and is on the World Health Organization's List of Essential Medicines. Additionally, it displays fluorescence enhancement upon binding to human serum albumin, making warfarin a prototype fluorescent probe in biology. Despite its biological significance, the current structural assignment of warfarin in aqueous solution is based on indirect evidence in organic solvents. Warfarin is known to exist in different isomeric forms—open-chain, hemiketal, and anionic forms—based on the solvent and pH. Moreover, warfarin displays a dual absorption feature in several solvents, which has been employed to study the ring-chain isomerism between its open-chain and hemiketal isomers. In this study, our pH-dependent experiments on warfarin and structurally constrained warfarin derivatives in aqueous solution demonstrate that the structural assignment of warfarin solely on the basis of its absorption spectrum is erroneous. Using a combination of steady-state and time-resolved spectroscopic experiments, along with quantum chemical calculations, we assign the observed dual absorption to two distinct $\pi \rightarrow \pi^*$ transitions in the 4-hydroxycoumarin moiety of warfarin. Furthermore, we unambiguously identify the isomeric form of warfarin that binds to human serum albumin in aqueous buffer.

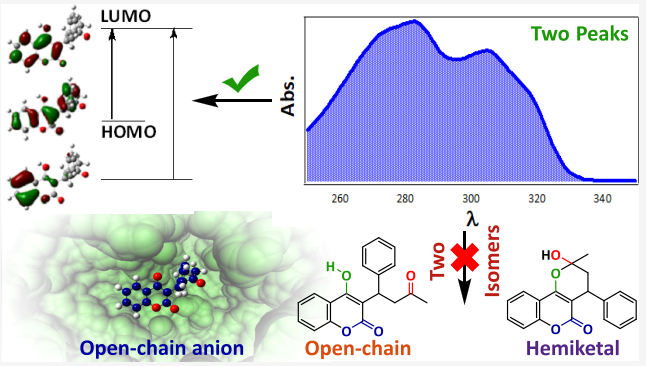

INTRODUCTION

Coumarin derivatives are of significant interest due to their pharmaceutical importance as well as their fluorescent properties. Warfarin, a coumarin derivative of clinical significance, is a highly potent anti-coagulant drug that reduces the risk of strokes and heart attacks by preventing blood clots in veins.[1−3] Moreover, warfarin binds to human serum albumin (HSA),[4] the most abundant protein in blood plasma that transports hormones, fatty acids, bilirubin, and drugs in the human body.[5,6] The high affinity and selectivity of warfarin toward HSA and the substantial increase in its fluorescence upon binding to the protein make warfarin a prototype fluorescent probe in biology.[7] Fluorescence lifetimes of warfarin in aqueous solution, free or bound to blood plasma proteins, have been correlated to blood coagulation.[8] Interestingly, warfarin is known to exist in various isomeric forms.[9−12] The conjugation between the functional groups gives rise to the coumarin and the chromone structures in various solvents (Figure 1).[13,14] Moreover, proximity of the hydroxyl and the carbonyl moieties allows open-chain and cyclic hemiketal conformations, leading to four possible isomers of warfarin. In addition, the deprotonated forms (anion) also contribute to the structural diversity of warfarin in water. Therefore, the structural determination of warfarin in water is important from the perspective of biological applications.[15]

Surprisingly, the current structural interpretation of warfarin in aqueous solution is based on indirect spectroscopic evidence in non-aqueous solvents. Nuclear magnetic resonance (NMR) studies in different organic solvents have indicated the predominance of the coumarin structural form over chromone.[13,16,17] In addition, the coexistence of hemiketal and open-chain isomeric forms has been suggested from NMR peak positions.[16−18] However, the structural details of warfarin in an aqueous medium are unavailable from NMR due to the low solubility of warfarin in water. More recently, absorption spectroscopy in organic solvents and in solvent mixtures has been employed in lieu of NMR to identify the warfarin isomers. The warfarin absorption spectrum consists of two overlapping peaks in the 250−350 nm range, which have been assigned to the hemiketal (~280 nm) and the open chain isomers (~310 nm).[19] Although the absorption experiments were not performed in an aqueous solution, several structural studies on the ring-chain isomerism as well as various biological applications of warfarin have used these absorption

Received: December 3, 2020
Revised: February 18, 2021
Published: March 17, 2021

https://doi.org/10.1021/acs.jpcb.0c10824
J. Phys. Chem. B 2021, 125, 2871−2878

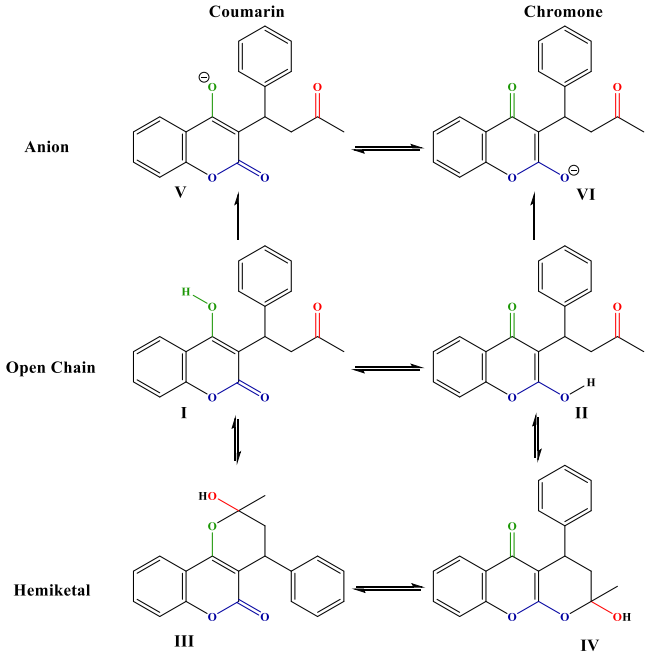

Figure 1. Possible isomers of warfarin: (**I**) coumarin open chain, (**II**) chromone open chain, (**III**) coumarin hemiketal, (**IV**) chromone hemiketal, (**V**) coumarin anionic, and (**VI**) chromone anionic. The hydroxyl, ketone, and ester functional groups are shown in green, red, and blue, respectively.

spectrum-based structural interpretations.[10,11,20−27] The interpretation gets even more ambiguous with another recent study suggesting that these two absorption peaks of warfarin arise not from the different isomeric forms but from $n \rightarrow \pi^*$ and $\pi \rightarrow \pi^*$ transitions.[23] The biological significance of warfarin and the existence of several coumarin-based drug molecules demand an unambiguous structural assignment in the aqueous medium.

In this report, we investigate the origin of the dual absorption of warfarin in aqueous solution using a combination of time-averaged and time-resolved spectroscopic experiments and quantum mechanical calculations. Absorption and emission experiments on warfarin in aqueous solutions at different pH values are performed. In addition, experiments are performed on warfarin derivatives with structural constraints such that only one of the isomeric forms is available for warfarin. Interestingly, we observe a similar dual absorption pattern for both the structurally constrained warfarin derivatives, irrespective of being restricted to one particular isomer. These results demonstrate that the lower and the higher wavelength transitions in the absorption spectrum of warfarin do not arise from two different structural isomers. This is further corroborated by steady-state emission spectroscopy. Our results show that the ring-chain isomerism of molecules structurally related to warfarin cannot be explained using the relative populations of the two absorption bands as they have been done in the past. Further, our results also show that the dual absorption is due to two distinct $\pi \rightarrow \pi^*$ transitions of warfarin. Quantum chemical calculations indicate that the dual absorption band arises due to distinct transitions to accessible excited states. The transitions take place from two energetically close occupied molecular orbitals (MOs) to the lowest unoccupied molecular orbital (LUMO) pertaining to the coumarin moiety of warfarin. Time-resolved emission spectroscopy on coumarin derivatives confirms that warfarin exists in its anionic form in water at a pH greater than 6.0. Further, experiments are performed in the presence of HSA to identify the isomer of warfarin that binds to the blood plasma protein in aqueous buffer. Our results reveal that warfarin adopts an open-chain anionic form when bound to HSA, independent of the pH of the aqueous buffer.

MATERIALS AND METHODS

Chemicals. Warfarin (analytical standard), 4-hydroxycoumarin (98%), pyranocoumarin (analytical standard), and HSA were purchased from Sigma-Aldrich, and their purity was checked using the high-performance liquid chromatography−mass spectrometry (HPLC-MS) technique. Methoxywarfarin and 4-methoxycoumarin were synthesized using the normal methylation method, and purity of the synthesized compounds was checked by NMR spectroscopy and the HPLC-MS technique.[28] All solvents were of spectroscopy grade (Sigma-Aldrich).

Spectroscopic Experiments. Absorption and fluorescence spectra were measured in a Shimadzu UV−vis−NIR (360^+) spectrophotometer and a PTI Quanta Master steady-state spectrofluorometer, respectively. A quartz cell of a 1 cm path length was used as the sample chamber. Freshly prepared ~60 μM solutions of warfarin and its related compounds were used for this purpose. Picosecond fluorescence dynamics studies of the fluorophore solutions were performed with a time-correlated single-photon counting (TCSPC) system employing a picosecond laser operating with λ_{ex} = 310 nm and a pulse width of ~50 ps.

Quantum Chemical Calculations. Geometries of 4-hydroxycoumarin, 4-methoxycoumarin, and different isomeric forms of warfarin were optimized using density functional theory (DFT) with the hybrid functional B3LYP[29,30] and the 6-31+G(d,p) basis set. The effect of the solvent was incorporated during geometry optimization using the SMD solvation model.[31] The calculation of transition energies and oscillator strengths of the higher singlet excited states were performed using time-dependent density functional theory (TDDFT) with the same functional and basis set. It was shown that transition energies calculated by the TDDFT method matched well with experimental values for coumarin derivatives.[32−35] Molecular orbital diagrams of all possible forms of every compound were computed at the Hartree−Fock (HF) level of theory with the 6-31+G(d,p) basis set. The equation-of-motion coupled-cluster singles and doubles (EOM-CCSD) method, with the same 6-31+G(d,p) basis set, was used to calculate accurate oscillator strengths of isolated 4-methoxycoumarin. The DFT, TDDFT, and HF calculations were performed using the Gaussian 09 program,[36] and the EOM-CCSD calculations were carried out using Molpro 2012.[37,38]

RESULTS AND DISCUSSION

The ground-state structures of different isomeric forms of warfarin in water are optimized using DFT (Table 1). We consider every possible structural conformer of warfarin to remove any bias reported in previous studies. The open-chain and the cyclic hemiketal coumarin structures (**I** and **III**) are found to be more stable than the corresponding chromone structures (**II** and **IV**). Moreover, in the case of any equilibrium between **I** and **III**, the equilibrium is expected to shift toward the lower energy hemiketal isomer. Estimation of

https://doi.org/10.1021/acs.jpcb.0c10824
J. Phys. Chem. B 2021, 125, 2871−2878

Table 1. Calculated Spectral Parameters for $S_0 \rightarrow S_1$ Electronic Transitions of Various Forms of Warfarin in Water (SMD Solvation Model) Using DFT and TDDFT B3LYP/6-31+G(d,p)

	open chain		hemiketal		anion
structure	I	II	III	IV	(V/VI)[a]
relative ground-state energy (kcal/mol)	3.6	10.6	0.0	8.0	288.4
absorption λ_{max} (nm)	316.7	309.7	303.1	309.7	319.3
oscillator strength (f)	0.56	0.03	0.66	0.04	0.44

[a]See the Supporting Information for details.

the $S_0 \rightarrow S_1$ transition wavelengths and the corresponding oscillator strengths further suggests that the chromone conformers are not only energetically unfavorable but also would not contribute to the absorption spectrum of warfarin. The structures **V** and **VI** corresponding to the warfarin anion are merely resonance structures, and thus, a single species of the deprotonated form of warfarin is present in solution at higher pH.

Absorption spectra of warfarin in aqueous solution show two distinct absorption peaks centered at ∼280 and ∼310 nm at lower pH (Figure 2a). An increase in the pH results in the decrease in the absorbance of the ∼280 nm peak along with a concomitant increase in the absorbance of the ∼310 nm peak.

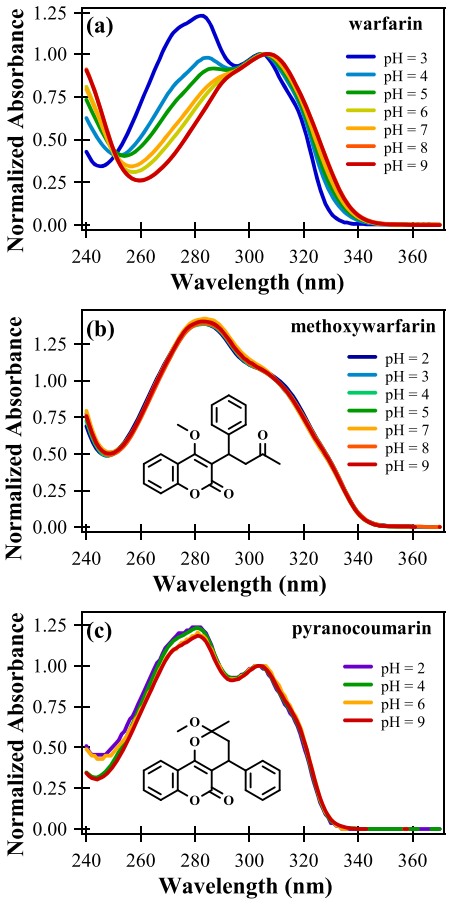

Figure 2. Normalized (at 310 nm) absorption spectra of (a) warfarin, (b) methoxywarfarin, and (c) pyranocoumarin in aqueous solution of different pH. The structures of methoxywarfarin and pyranocoumarin are shown along with the spectra.

Moreover, a small red shift is observed in the band at ∼310 nm for pH values greater than 5. On the basis of previous structural assignments (Figure S1 in the Supporting Information), the dual absorption pattern in water can be speculated to arise from the open chain (∼310 nm) and the hemiketal isomers (∼280 nm).[19,20] Although this speculation may appear qualitatively consistent with our calculated wavelengths, confounding results are obtained when control experiments are performed on structurally constrained warfarin derivatives.

Two structurally constrained warfarin derivatives, methoxywarfarin and pyranocoumarin (structures in Figure 2b and Figure 2c, respectively), are chosen, which by virtue of their structures, are restricted to exclusively open-chain and hemiketal conformers, respectively. Surprisingly, similar to warfarin, both methoxywarfarin and pyranocoumarin have dual absorptions at ∼280 and ∼310 nm (Figure 2b and Figure 2c, respectively), irrespective of their confinement to one specific isomeric form. However, unlike warfarin, the absorption spectra of methoxywarfarin and pyranocoumarin do not show any pH dependence. The inability of methoxywarfarin and pyranocoumarin to convert to the anionic form is the likely explanation for the invariance of the absorption spectra with changing pH. As the stability of pyranocoumarin may be debatable in acidic solution (see the Supporting Information for details), absorption experiments are further performed in non-aqueous solvents to confirm the dual absorption pattern of pyranocoumarin (Figure S2 in the Supporting Information). These observations in structurally constrained warfarin derivatives are in conflict with the earlier structural assignments of warfarin on the sole basis of the absorption spectrum.[19] This gives rise to the following question: what then is the origin of the two bands?

A recent report has mentioned that the dual absorption of warfarin arises from $n \rightarrow \pi^*$ and $\pi \rightarrow \pi^*$ transitions.[23] As a single carbon−carbon bond fission of warfarin results in 4-hydroxycoumarin and phenylbutanone (structures are shown in Figure 3a) without any change in the conjugation length, the absorption spectrum of warfarin can be considered to be a combination of the absorption spectra of the two moieties. Negligible absorption due to the $n \rightarrow \pi^*$ transition of the keto-carbonyl group at ∼260 nm is observed for phenylbutanone (Figure 3a). The absorption spectrum of 4-hydroxycoumarin (Figure 3a,b) shows similar spectral signatures and pH dependence as that of warfarin. pH-independent dual absorption of 4-methoxycoumarin (Figure 3c), similar to that of 4-methoxywarfarin, further suggests that the single absorption band at higher pH in both warfarin and 4-hydroxycoumarin (pK_a of 4.1)[15] arises due to the anionic species. More importantly, both the transition frequency and the weak intensity of the $n \rightarrow \pi^*$ absorption in phenylbutanone suggest that the $n \rightarrow \pi^*$ transition does not contribute to the dual absorption of warfarin. These results clearly indicate that the 4-hydroxycoumarin moiety of warfarin is solely responsible for the dual absorption pattern. This is a significant conclusion, although the assignment of the two bands still remains unresolved.

In a previous report on coumarin, the dual absorption was hypothesized to arise from HOMO → LUMO and HOMO-1 → LUMO transitions.[39,40] As our results suggest that the dual absorption profile of warfarin arises exclusively from the 4-hydroxycoumarin moiety, TDDFT calculations are performed for all possible Franck−Condon transitions on the optimized

https://doi.org/10.1021/acs.jpcb.0c10824
J. Phys. Chem. B 2021, 125, 2871−2878

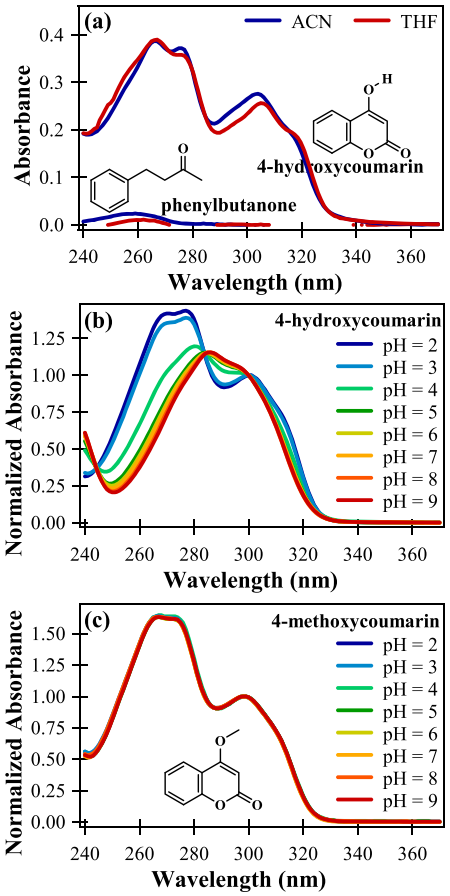

Figure 3. Absorption spectra of (a) phenylbutanone and 4-hydroxycoumarin in ACN and THF; normalized absorption spectra of (b) 4-hydroxycoumarin and (c) 4-methoxycoumarin in aqueous solutions of different pH. The structures of phenylbutanone, 4-hydroxycoumarin, and 4-methoxycoumarin are shown along with the spectra.

geometries of 4-hydroxycoumarin (neutral and anionic), 4-methoxycoumarin, and warfarin (all coumarin-type isomers). The HF molecular orbitals (MOs) are also computed. Schematic representations of all possible transitions in 4-hydroxycoumarin, its anion and 4-methoxycoumarin (within 260−340 nm), the corresponding oscillator strengths (f), and the MOs are shown in Figure 4a−c and Figure S3a−c (see the Supporting Information). Additional schematic representations from similar calculations on different coumarin-type isomers of warfarin in the range of experimental absorption are shown in Figure 4d−f and Figure S3d−f (see the Supporting Information). Figure 4 and Figure S3 clearly show that only π orbitals are involved in every transition. Furthermore, the n-type orbitals are quite buried and the first n-type orbital below the highest occupied molecular orbital (HOMO) is HOMO 5 or HOMO-6, as presented in Figures S4 and S5 in the Supporting Information. Therefore, these calculations provide further theoretical support to disregard the contribution of the $n \rightarrow \pi^*$ transition to the absorption spectrum. According to energy profile diagrams, HOMO → LUMO, HOMO-1 → LUMO $\pi \rightarrow \pi^*$ transitions contribute to the dual absorption of 4-hydroxycoumarin and 4-methoxycoumarin. The dual absorption nature of warfarin at lower pH can also be explained to arise from transitions originating from distinct but energetically close occupied orbitals to the LUMO. The DFT calculated wavelengths agree well with those obtained from experiments. Theoretically, thecalculated oscillator strength corresponding to any transition is comparable with the experimentally observed optical density. For deprotonated warfarin and 4-hydroxycoumarin, oscillator strengths are relatively high for HOMO → LUMO transitions, while they are small for other higher energy transitions. These results explain the experimentally observed single absorption nature of the anionic species at high pH. In addition, the calculated absorption wavelength is the highest for the warfarin anion, which also explains the red shift observed in the warfarin absorption spectrum with an increase in pH.

The only observation that is not reproduced by the TDDFT calculations is the relative intensities of the lower and higher wavelength transitions in the experimental absorption spectra of warfarin and 4-hydroxycoumarin at low pH. Therefore, a more accurate, albeit computationally expensive method, EOM-CCSD, has been used to perform calculations on 4-methoxycoumarin to address this issue (Table 2).[41] 4-Methoxycoumarin is selected instead of warfarin to reduce computational cost as well as to restrict any contribution from the anionic form in the dual absorption. This calculation has been carried out in the gas phase because the inclusion of solvent effects increases computational costs significantly; moreover, EOM-CCSD calculations with continuum solvation models are known to have large errors.[42] The oscillator strengths predicted by EOM-CCSD are remarkably consistent with experimental absorbance. The absolute values of the excitation energies predicted by EOM-CCSD are higher than those predicted by TDDFT and the experiment, and this is possibly due to cancellation of errors in TDDFT and because EOM-CCSD calculations are performed for the isolated molecule corresponding to the gas phase, while the experimental spectrum is obtained in solution.

To validate the theoretical predictions, steady-state and time-resolved emission studies are performed on warfarin. In agreement with the earlier reports, emission bands, independent of the excitation wavelengths, are observed at ∼356 and ∼390 nm at pH = 3 and 9, respectively (Figure 5a and Figure 5b, respectively).[10,19,27] If warfarin exists as different structural isomers, then multiple distinct emission bands are expected. The single emission band supports the theoretical prediction that the dual absorption arises not from structural isomers but rather due to excitations from two distinct energetically accessible states. As radiative emission occurs exclusively for the $S_1 \rightarrow S_0$ transition, any fluorophore excited to S_2 (second excited singlet state) would initially decay to S_1 through internal conversion. This explains the single emission band of warfarin at 356 nm, irrespective of exciting the molecule to S_2 (280 nm) or S_1 (310 nm). On the other hand, at pH = 9, the red-shifted single emission peak at 392 nm is the emission of the warfarin anion. DFT calculations performed on excited-state structures of warfarin (Table S1 in the Supporting Information) agree well with the experimental results.

Earlier studies, limited by instrumental resolution, have speculated ultrafast excited-state dynamics of warfarin to be responsible for the single emission peak in steady-state fluorescence spectra.[10,19,27] Time-resolved emission experiments on warfarin at pH = 3 and 9 with λ_{ex} = 310 nm are performed. Time profiles, collected at several wavelengths across the steady-state fluorescence spectra (Figure 5c,d), exhibit a uniform decay rate at pH = 3, irrespective of emission wavelengths, indicating the absence of any excited-state

https://doi.org/10.1021/acs.jpcb.0c10824
J. Phys. Chem. B 2021, 125, 2871−2878

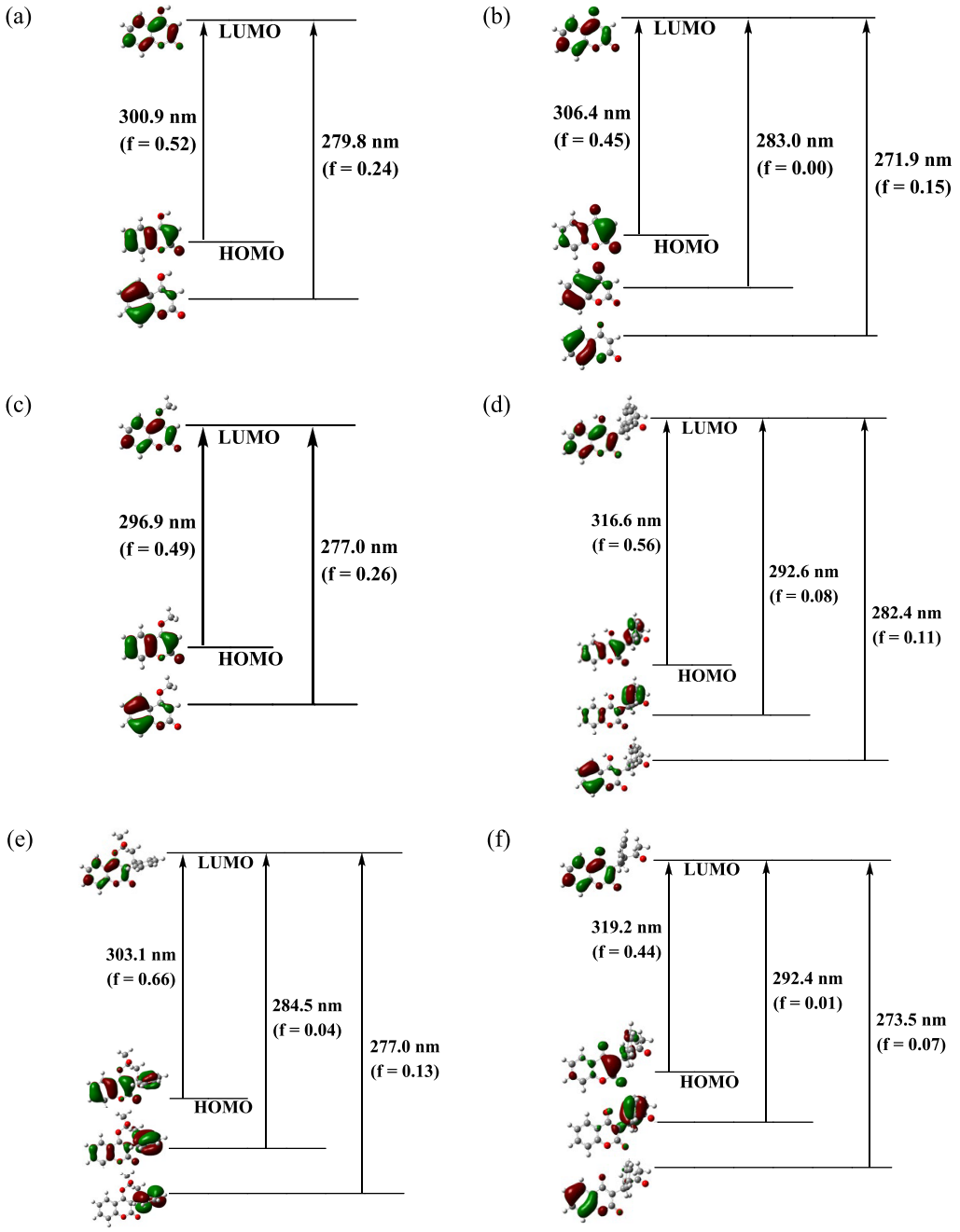

Figure 4. Energy level diagrams for (a) 4-hydroxycoumarin and (b) its anion, (c) 4-methoxycoumarin, and warfarin in its (d) open-chain, (e) cyclic hemiketal, and (f) anionic forms in the aqueous medium (SMD solvation model). Molecular orbitals are calculated at the HF/6-31+G(d,p) level of theory, while the excitation energies are calculated using the TDDFT B3LYP/6-31+G(d,p) method.

Table 2. Calculated Spectral Parameters for Electronic Transitions of 4-Methoxycoumarin in Vacuum at the EOM-CCSD/6-31+G(d,p) Level of Theory

	absorption λ_{max} (nm)	oscillator strength (f)	predominant orbitals involved
first allowed transition	272.0	0.10	HOMO → LUMO
second allowed transition	235.1	0.24	(HOMO-1) → LUMO and HOMO → LUMO

dynamic process of a time scale slower than 50 ps in warfarin. A single exponential fit to the emission time profile at 360 nm provides the fluorescence lifetime of warfarin at pH = 3 to be ~55 ps. Emission time profiles of deprotonated warfarin at pH = 9 also indicate a constant, yet slower, decay rate of ~125 ps, irrespective of the emission wavelength. These observed emission lifetimes are consistent with the fluorescence quantum yields (φ) at pH = 3 ($\varphi = 2.71 \times 10^{-3}$) and 9 ($\varphi = 4.77 \times 10^{-3}$), calculated using anthracene as a standard reference compound at its excitation wavelength (305 nm) in cyclohexane ($\varphi = 0.36$).[43] The calculated non-radiative decay rate, found to be ~2.3 times slower at pH = 9, further validates the presence of the anionic species at higher pH. The rigidity due to extended conjugation in the anion suppresses the non-radiative decay channel, thereby increasing the emission quantum yield as well as emission lifetime of deprotonated

https://doi.org/10.1021/acs.jpcb.0c10824
J. Phys. Chem. B 2021, 125, 2871−2878

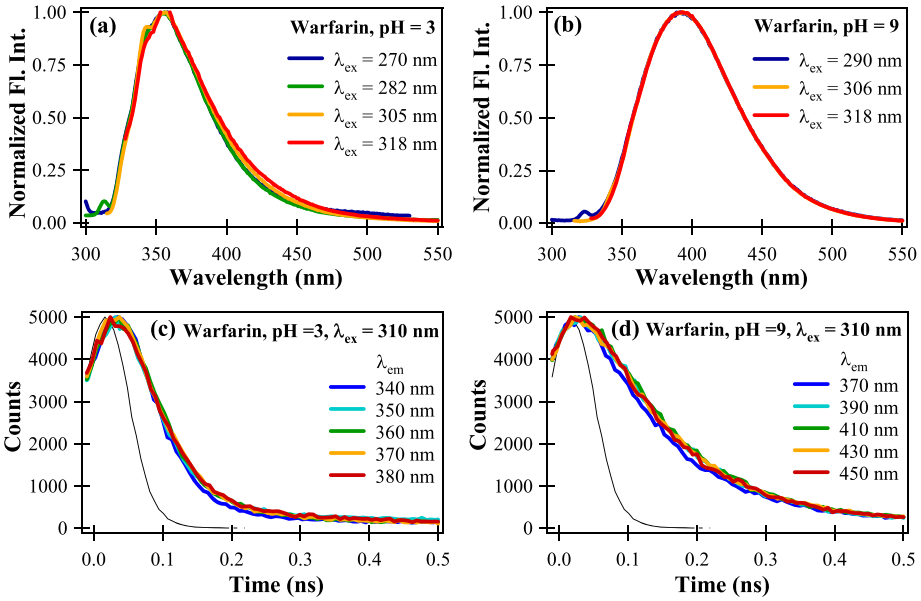

Figure 5. Normalized emission spectra of warfarin in (a) pH = 3 and (b) pH = 9 at different excitation wavelengths.Time-resolved fluorescence profiles of warfarin in (c) pH = 3 and (d) pH = 9 at different emission wavelengths, as indicated (λ_{ex} = 310 nm). Black solid line represents instrumental response function (IRF).

warfarin. As discussed earlier, our theoretical calculations indicate that a single species of deprotonated warfarin is present in solution at higher pH.

Since warfarin is used as an anti-coagulant drug as well as a prototype fluorescent probe in biology, it is imperative to ascertain which isomeric form of warfarin binds to HSA. The reported X-ray diffraction data of the crystal structure of the warfarin-HSA complex are consistent with the open-chain form of the warfarin molecule;[44] however, the protonated or deprotonated status of warfarin, when bound to HSA, cannot be determined from X-ray diffraction. To determine the protonation status of warfarin in the enzyme environment, we perform absorption and emission experiments of the warfarin-HSA complex at three different pH values (3, 7.4, and 9). The absorption spectrum at any pH shows a single absorption band at ∼310 nm (Figure S6a in the Supporting Information). The emission spectrum shows a single fluorescence peak at ∼382 nm (Figure S6b in the Supporting Information). Interestingly, the absorption as well as emission spectra of HSA-bound warfarin is almost independent of pH. Close resemblance of the absorption spectra of warfarin, when bound to HSA, with its deprotonated form indicates that warfarin is present in the open-chain anionic form in the HSA binding pocket. However, the emission spectrum shows an ∼10 nm blue shift from that obtained for deprotonated warfarin in aqueous solution (pH = 9). The high microviscosity of the binding pocket, as compared to the surrounding, can explain the blue shift of the emission maximum. In a previous report,[45] a gradual blue shift of warfarin emission maxima has been reported with increasing viscosity of the solvent. Above experimental evidence also suggest that the pH of the protein solution has minimal effect on the warfarin binding site and that the warfarin molecule is confined in the protein pocket.

CONCLUSIONS

Using a combined theoretical and experimental study of warfarin, we confirm that the coumarin moiety of warfarin is solely responsible for the absorption spectrum of warfarin in its aqueous form. We demonstrate that the dual absorption feature in the absorption spectrum is not indicative of the presence of multiple isomeric structures of warfarin in solution but rather due to excitations arising from two closely spaced occupied molecular orbitals terminating at the lowest unoccupied molecular orbital. Our study also illustrates that the ring-chain isomerism of molecules structurally similar to warfarin, as reported in previous studies, cannot be explained using the spectral features of the warfarin absorption spectrum. Further, this report decisively eliminates the possibility of the $n \rightarrow \pi^*$ transition contributing to the dual absorption feature of warfarin. The steady-state and the time-resolved emission experiments provide additional support to distinguish between the neutral and the anionic isomers of warfarin. Further, these results allow us to determine that warfarin exists in the open-chain anionic form in the active site of HSA. Finally, as the coumarin moiety, which mostly contributes to the absorption and emission spectrum of warfarin, is present in many drugs, our study will be helpful in examining various drug−receptor interactions.

ASSOCIATED CONTENT

Supporting Information

The Supporting Information is available free of charge at https://pubs.acs.org/doi/10.1021/acs.jpcb.0c10824.

Structure of the warfarin anion, absorption spectra of warfarin and pyranocoumarin, pyranocoumarin in acidic pH solution, calculated spectral parameters of warfarin, and absorption and emission spectra of the warfarin-HSA complex (PDF)

AUTHOR INFORMATION

Corresponding Authors

Anirban Hazra − *Department of Chemistry, Indian Institute of Science Education and Research, Pune 411008, India;* orcid.org/0000-0003-2012-381X; Email: ahazra@iiserpune.ac.in

https://doi.org/10.1021/acs.jpcb.0c10824
J. Phys. Chem. B 2021, 125, 2871−2878

Sayan Bagchi − *Physical and Materials Chemistry Division, CSIR-National Chemical Laboratory, Pune 411008, India; Academy of Scientific and Innovative Research (AcSIR), Ghaziabad 201002, India;* orcid.org/0000-0001-6932-3113; Email: s.bagchi@ncl.res.in

Authors

Sushil S. Sakpal − *Physical and Materials Chemistry Division, CSIR-National Chemical Laboratory, Pune 411008, India; Academy of Scientific and Innovative Research (AcSIR), Ghaziabad 201002, India*

Deborin Ghosh − *Physical and Materials Chemistry Division, CSIR-National Chemical Laboratory, Pune 411008, India*

Meghna A. Manae − *Department of Chemistry, Indian Institute of Science Education and Research, Pune 411008, India*

Complete contact information is available at: https://pubs.acs.org/10.1021/acs.jpcb.0c10824

Author Contributions

#S.S.S. and D.G. contributed equally to this work.

Notes

The authors declare no competing financial interest.

■ ACKNOWLEDGMENTS

This work was financially supported by SERB India (EMR/2016/000576). D.G. acknowledges SERB India for the NPDF fellowship (PDF/2018/000046). S.S.S. acknowledges UGC for the fellowship. The authors would like to thank Prof. Anindya Datta, IIT Bombay, for help with the time-resolved fluorescence experiments.

■ REFERENCES

(1) Li, T.; Chang, C. Y.; Jin, D. Y.; Lin, P. J.; Khvorova, A.; Stafford, D. W. Identification of the gene for vitamin K epoxide reductase. *Nature* **2004**, *427*, 541−544.

(2) Rost, S.; Fregin, A.; Ivaskevicius, V.; Conzelmann, E.; Hörtnagel, K.; Pelz, H.-J.; Lappegard, K.; Seifried, E.; Scharrer, I.; Tuddenham, E. G.; Müller, C. R.; Strom, T. M.; Oldenburg, J. Mutations in VKORC1 cause warfarin resistance and multiple coagulation factor deficiency type 2. *Nature* **2004**, *427*, 537−541.

(3) Mohr, J. P.; Thompson, J. L. P.; Lazar, R. M.; Levin, B.; Sacco, R. L.; Furie, K. L.; Kistler, J. P.; Albers, G. W.; Pettigrew, L. C.; Adams, H. P., Jr.; Jackson, C. M.; Pullicino, P. A comparison of warfarin and aspirin for the prevention of recurrent ischemic stroke. *N. Engl. J. Med.* **2001**, *345*, 1444−1451.

(4) Peyrin, E.; Guillaume, Y. C.; Guinchard, C. Characterization of Solute Binding at Human Serum Albumin Site II and its Geometry Using a Biochromatographic Approach. *Biophys. J.* **1999**, *77*, 1206−1212.

(5) Liu, R.; Perez-Aguilar, J. M.; Liang, D.; Saven, J. G. Binding Site and Affinity Prediction of General Anesthetics to Protein Targets Using Docking. *Anesth. Analg.* **2012**, *114*, 947−955.

(6) Nicholson, J. P.; Wolmarans, M. R.; Park, G. R. The role of albumin in critical illness. *Br. J. Anaesth.* **2000**, *85*, 599−610.

(7) CF, C. Optical studies of drug-protein complexes. IV. The interaction of warfarin and dicoumarol with human serum albumin. *Mol. Pharmacol.* **1970**, *1*, 1−12.

(8) Rosengren, A. M.; Karlsson, B. C. G.; Nicholls, I. A. Monitoring the distribution of warfarin in blood plasma. *ACS Med. Chem. Lett.* **2012**, *3*, 650−652.

(9) Smirnova, T. D.; Nevryueva, N. V.; Shtykov, S. N.; Kochubei, V. I.; Zhemerichkin, D. A. Determination of warfarin by sensitized fluorescence using organized media. *J. Anal. Chem.* **2009**, *64*, 1114−1119.

(10) Al-Dubaili, N.; Saleh, N. Sequestration Effect on the Open-Cyclic Switchable Property of Warfarin Induced by Cyclodextrin: Time-Resolved Fluorescence Study. *Molecules* **2017**, *22*, 1326.

(11) Vasquez, J. M.; Vu, A.; Schultz, J. S.; Vullev, V. I. Fluorescence enhancement of warfarin induced by interaction with beta-cyclodextrin. *Biotechnol. Prog.* **2009**, *25*, 906−914.

(12) Otagiri, M.; Imai, T.; Koinuma, H.; Matsumoto, U. Spectroscopic study of the interaction of coumarin anticoagulant drugs with polyvinylpyrrolidone. *J. Pharm. Biomed. Anal.* **1989**, *7*, 929−935.

(13) Valente, E. J.; Lingafelter, E. C.; Porter, W. R.; Trager, W. F. Structure of warfarin in solution. *J. Med. Chem.* **1977**, *20*, 1489−1493.

(14) Valente, E. J.; Porter, W. R.; Trager, W. F. Conformations of selected 3-substituted 4-hydroxycoumarins in solution by nuclear magnetic resonance. Warfarin and phenprocoumon. *J. Med. Chem.* **1978**, *21*, 231−234.

(15) Nowak, P. M.; Sagan, F.; Mitoraj, M. P. Origin of Remarkably Different Acidity of Hydroxycoumarins—Joint Experimental and Theoretical Studies. *J. Phys. Chem. B* **2017**, *121*, 4554−4561.

(16) Giannini, D. D.; Chan, K. K.; Roberts, J. D. Carbon-13 Nuclear Magnetic Resonance Spectroscopy. Structure of the Anticoagulant Warfarin and Related Compounds in Solution. *Proc. Natl. Acad. Sci. U. S. A.* **1974**, *71*, 4221−4223.

(17) Pisklak, M.; Maciejewska, D.; Herold, F.; Wawer, I. Solid state structure of coumarin anticoagulants: warfarin and sintrom. 13C CPMAS NMR and GIAO DFT calculations. *J. Mol. Struct.* **2003**, *649*, 169−176.

(18) Guasch, L.; Peach, M. L.; Nicklaus, M. C. Tautomerism of Warfarin: Combined Chemoinformatics, Quantum Chemical, and NMR Investigation. *J. Org. Chem.* **2015**, *80*, 9900−9909.

(19) Karlsson, B. C. G.; Rosengren, A. M.; Andersson, P. O.; Nicholls, I. A. The Spectrophysics of Warfarin: Implications for Protein Binding. *J. Phys. Chem. B* **2007**, *111*, 10520−10528.

(20) Rosengren, A. M.; Karlsson, B. C. G. Spectroscopic evidence for the presence of the cyclic hemiketal form of warfarin in aqueous solution: Consequences for bioavailability. *Biochem. Biophys. Res. Commun.* **2011**, *407*, 318−320.

(21) Guasch, L.; Sitzmann, M.; Nicklaus, M. C. Enumeration of Ring−Chain Tautomers Based on SMIRKS Rules. *J. Chem. Inf. Model.* **2014**, *54*, 2423−2432.

(22) Kumar, P.; Kumar, V.; Gupta, R. Detection of the anticoagulant drug warfarin by palladium complexes. *Dalton Trans.* **2017**, *46*, 10205−10209.

(23) Kumari, R.; Nath, M. Synthesis and characterization of novel trimethyltin(IV) and tributylltin(IV) complexes of anticoagulant, WARFARIN: Potential DNA binding and plasmid cleaving agents. *Inorg. Chem. Commun.* **2018**, *95*, 40−46.

(24) Dar, A. A.; Chat, O. A. Cosolubilization of Coumarin30 and Warfarin in Cationic, Anionic, and Nonionic Micelles: A Micelle−Water Interfacial Charge Dependent FRET. *J. Phys. Chem. B* **2015**, *119*, 11632−11642.

(25) Karlsson, B. C. G.; Olsson, G. D.; Friedman, R.; Rosengren, A. M.; Henschel, H.; Nicholls, I. A. How Warfarin's Structural Diversity Influences Its Phospholipid Bilayer Membrane Permeation. *J. Phys. Chem. B* **2013**, *117*, 2384−2395.

(26) Malde, A. K.; Stroet, M.; Caron, B.; Visscher, K. M.; Mark, A. E. Predicting the Prevalence of Alternative Warfarin Tautomers in Solution. *J. Chem. Theory Comput.* **2018**, *14*, 4405−4415.

(27) Karlsson, B. C. G.; Rosengren, A. M.; Andersson, P. O.; Nicholls, I. A. Molecular Insights on the Two Fluorescence Lifetimes Displayed by Warfarin from Fluorescence Anisotropy and Molecular Dynamics Studies. *J. Phys. Chem. B* **2009**, *113*, 7945−7949.

(28) Chou, P. T.; Martinez, M. L.; Clements, J. H. Reversal of Excitation Behavior of Proton-Transfer vs. Charge-Transfer by Dielectric Perturbation of Electronic Manifolds. *J. Phys. Chem.* **1993**, *97*, 2618−2622.

(29) Lee, C.; Yang, W.; Parr, R. G. Development of the Colle-Salvetti correlation-energy formula into a functional of the electron density. *Phys. Rev. B* **1988**, *37*, 785−789.

(30) Becke, A. D. Density-functional thermochemistry. III. The role of exact exchange. *J. Chem. Phys.* **1993**, *98*, 5648−5652.
(31) Marenich, A. V.; Cramer, C. J.; Truhlar, D. G. Universal Solvation Model Based on Solute Electron Density and on a Continuum Model of the Solvent Defined by the Bulk Dielectric Constant and Atomic Surface Tensions. *J. Phys. Chem. B* **2009**, *113*, 6378−6396.
(32) Jacquemin, D.; Perpète, E. A.; Assfeld, X.; Scalmani, G.; Frisch, M. J.; Adamo, C. The geometries, absorption and fluorescence wavelengths of solvated fluorescent coumarins: A CIS and TD-DFT comparative study. *Chem. Phys. Lett.* **2007**, *438*, 208−212.
(33) Cerón-Carrasco, J. P.; Fanuel, M.; Charaf-Eddin, A.; Jacquemin, D. Interplay between solvent models and predicted optical spectra: A TD-DFT study of 7-OH-coumarin. *Chem. Phys. Lett.* **2013**, *556*, 122−126.
(34) Jacquemin, D.; Perpète, E. A.; Scuseria, G. E.; Ciofini, I.; Adamo, C. TD-DFT Performance for the Visible Absorption Spectra of Organic Dyes: Conventional versus Long-Range Hybrids. *J. Chem. Theory Comput.* **2008**, *4*, 123−135.
(35) Jacquemin, D.; Planchat, A.; Adamo, C.; Mennucci, B. TD-DFT Assessment of Functionals for Optical 0−0 Transitions in Solvated Dyes. *J. Chem. Theory Comput.* **2012**, *8*, 2359−2372.
(36) Frisch, M. J.; Trucks, G. W.; Schlegel, H. B.; Scuseria, G. E.; Robb, M. A.; Cheeseman, J. R.; Scalmani, G.; Barone, V.; Mennucci, B.; Petersson, G. A. et al., *Gaussian 09* Revision A.01, Gaussian, Inc.: Wallingford CT 2009.
(37) Werner, H.-J.; Knowles, P. J.; Knizia, G.; Manby, F. R.; Schütz, M.; Celani, P.; Korona, T.; Lindh, R.; Mitrushenkov, A.; Rauhut, G. *version 2010.1, a package of ab initio programs* 2010.
(38) Werner, H.-J.; Knowles, P. J.; Knizia, G.; Manby, F. R.; Schütz, M. Molpro: a general-purpose quantum chemistry program package. *WIREs Comput. Mol. Sci.* **2012**, *2*, 242−253.
(39) Moore, T. A.; Harter, M. L.; Song, P.-S. Ultraviolet spectra of coumarins and psoralens. *J. Mol. Spectrosc.* **1971**, *40*, 144−157.
(40) Song, P.-S.; Gordon, W. H., III Spectroscopic study of the excited states of coumarin. *J. Phys. Chem.* **1970**, *74*, 4234−4240.
(41) Caricato, M.; Trucks, G. W.; Frisch, M. J.; Wiberg, K. B. Oscillator Strength: How Does TDDFT Compare to EOM-CCSD? *J. Chem. Theory Comput.* **2011**, *7*, 456−466.
(42) Ren, S.; Harms, J.; Caricato, M. An EOM-CCSD-PCM Benchmark for Electronic Excitation Energies of Solvated Molecules. *J. Chem. Theory Comput.* **2017**, *13*, 117−124.
(43) Berlman, I. B., *Handbook of Fluorescence Spectra of Aromatic Molecules;* Academic Press: New York, 1971.
(44) Petitpas, I.; Bhattacharya, A. A.; Twine, S.; East, M.; Curry, S. Crystal Structure Analysis of Warfarin Binding to Human Serum Albumin: ANATOMY OF DRUG SITE I. *J. Biol. Chem.* **2001**, *276*, 22804−22809.
(45) Kasai-Morita, S.; Horie, T.; Awazu, S. Influence of the N-B transition of human serum albumin on the structure of the warfarin-binding site. *Biochim. Biophys. Acta* **1987**, *915*, 277−283.

https://doi.org/10.1021/acs.jpcb.0c10824
J. Phys. Chem. B 2021, 125, 2871−2878